Computer Simulations of The Dynamics of Asymmetric Dimers in Optical Traps of Varying Polarization

Daniel MacIver, Praveen Parthasarathi*, Leo Lue, Jan Sefcik, and Mark Haw
Department of Chemical and Process Engineering, University of Strathclyde, Glasgow, United Kingdom
*praveen.parthasarathi@strath.ac.uk

Abstract: We report on computer simulations of the equilibrium positions, dynamics, and orientations of asymmetric microsphere dimers of varying size ratios in a single Gaussian beam Optical Trap of varying laser-polarization. We show that in case of a dimer, the trapping force profile deviates very quickly from a simple linear sum of forces on individual spheres as the size of the second sphere is increased and shows multiple axial-equilibrium positions for the case of larger bead closer to the laser focus as against the case of a smaller bead closer to the focus. Furthermore, we also investigate sustained rotations of dimers about their long-axis when trapped in a circularly polarized laser and study the effect of size-asymmetry on rotation rates. We hope these studies might be useful to researchers investigating colloidal aggregation and nucleation in optical traps and we also make a case for optically trapped dimers as microrotors.

1. Introduction

Ever since their invention in 1986 by Arthur Ashkin [1], Optical Traps or Optical Tweezers (OT) have been used extensively in colloidal physics [2-4]. Of particular interest has been the use of a single trapped microsphere as a tracer to probe the rheological properties of the fluid of suspension [5]. However, while working with dense colloidal suspensions, one often ends up trapping more than one microbead in a Gaussian beam OT. Li and Arlt [6] studied the case of two microspheres trapped in a single OT and opined that multiple trapped beads could be mistaken for a single trapped bead with altered trap stiffness. Theoretical studies on the case of two trapped microspheres by Xu et.al., [7] employed a ray-optics based model to show that the two trapped beads are brought into physical contact with each other by optical forces and they also calculated the axial equilibrium positions of the two trapped beads as a function of their size. Sheng-Hua et al [8] assumed that the two trapped beads experience different trap stiffnesses and went on to show that the trapped beads collide. Experiments in [9] confirmed that the two trapped beads indeed experience different trap stiffnesses when trapped in a single Gaussian beam OT.

Besides multiple trapped beads, trapping and dynamics of asymmetric shapes have generated a lot of interest. Mihiretie et.al., [10] studied the trapping of ellipsoidal microparticles and found that particles of aspect ratio ‘k’ greater than 3 and less than 0.3 exhibited oscillatory dynamics with a coupling between translation and rotation in the trap and those with aspect ratio outside this range exhibited less pronounced oscillations with the major axis pre-dominantly pointed along the laser propagation direction. Cao et.al., [11] performed T-Matrix based simulations of the trapping dynamics of nanowires and microcylinders in the Rayleigh regime and found that polarization dictated the final equilibrium orientation with the nanowires equilibrating with a large tilt angle about the laser propagation direction when the beam was linearly polarized and along the beam propagation direction in circularly polarized traps. Chetana D et, al., [12] increased the complexity of the problem by considering an object with both shape as well as optical anisotropy in the form of a chicken Red Blood Cell (cRBC) and showed that the trapping dynamics and the final equilibrium orientation of the cRBC was decided by the beam polarization with the cell showing a dual reorientation behaviour in a linearly polarized trap and a partial second reorientation in a circularly polarized trap.
In this work, we extend the Brownian dynamical simulations carried out by Vigilante et.al., [13] to the case of asymmetric dimers. We begin by showing that the optical force on a microsphere-dimer quickly deviates from a simple sum of forces on two spheres and thus underscore the relevance of the choice

of *mstm*, a well-established package for calculating light scattering from a cluster of spheres [14] and within it *ott*, a well-established toolbox for computing forces and torques in an OT [15]. We show validations of the dynamical simulations for the case of a single trapped bead in both linear and circularly polarized traps with the suspension medium being water at room temperature. We then reproduce the results for dynamics of a symmetric dimer in [13] as further validation of our codes. We organize our results into 3 sections with the focus on axial and orientation trapping equilibria for different size-ratios of the dimers in the first section, determinations of equilibrium orientations and equilibrium positions of various dimers with varied initial conditions of orientation and position in linearly and circularly polarised traps, Finally, we report interesting rotational dynamics of dimers seen only when the light is not linearly polarised. We hope that our results could inform studies on colloidal aggregation and help design rotors for use in applications such as lab-on-a-chip and micromachines.

2. Methods

Simulating motion within an optical trap

We assume the dimers to be low-Reynold's number objects and write down their dynamics within the trap using the Langevin equation:

$$\frac{dx(t)}{dt} = \frac{F(x)}{\gamma} + \sqrt{2D}\eta_x(t)$$

Where F(x) is the optical force directed towards the focal point of the laser However, this is only accurate when close to the equilibrium position, if we wish to probe the phase space we need a means of computing the optical forces for any position or orientation. Fortunately, Vigilante et al [13] have already built the ground work for simulating multi-sphere trapping. This work is an extension of the simulation work conducted by [13] into multi-sphere objects; their paper already has an excellent breakdown of the mathematics that go into calculating the optical and hydrodynamic forces, as such we will only refer to the mathematical methodology when necessary or when our work diverges from [13]. For simulating asymmetric objects, in which translation and rotation dynamics are coupled, it is useful to have two separate reference systems: The laboratory frame, which refers to the larger system

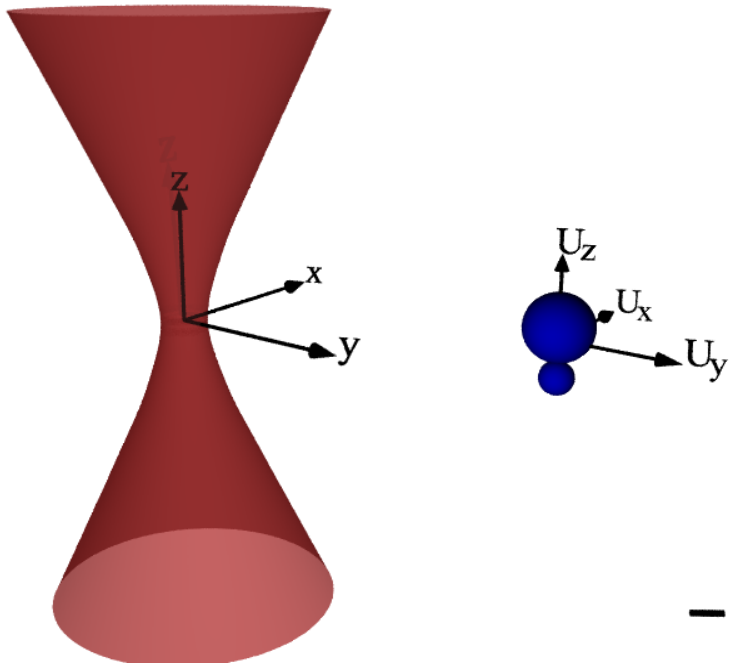

Figure 1: Render of trapping beam and a 1:2 dimer with respective laboratory frame and particle reference frame. The laboratory frame origin is set at the focal point of the Gaussian beam. The particle reference axes are used to set the relative positions of each sphere, the axes are centred on dimer's centre of diffusion and used to describe the dimer's orientation. Scale bar in bottom right corner represnts 1 µm.

centered at the focal point of the trapping laser; and the particle reference frame which defines the positions of individual spheres, in the case of a dimer the spheres are positioned so that the center of diffusion is at the origin of the particle reference frame. The axis of the particle reference frame is used to define the orientation of the dimer; with U_z intersecting the centers of the two spheres; any rotations are applied to the reference axis so that the orientation is preserved.

The code combines the optical force calculation code from Optical Tweezer Toolbox (*ott*) and the T-matrix calculations from Multi-Sphere T-Matrix (*mstm*); after initializing the target object *mstm* calculates its T-matrix before returning the T-matrix object to *ott* to calculate the optical forces and torques as well as the hydrodynamic forces due to the Brownian force. This circumvents the limitations of both *ott* and *mstm*; mainly that *ott* struggles to model the T-matrix of multi-shape objects that experience internal scattering, and that *mstm* cannot model scattering from lasers with a high NA commonly used in optical trapping. After calculating the total force and torque in the laboratory frame they are scaled down to the particle reference frame, where the reference axis is rotated appropriately before then displacing the object in the laboratory frame to update its position.
The Brownian OT code from Vigilante has code for simulating both dimers, and sphere clusters; the former is only capable of processing symmetric dimers with no ability to freely tune the size of each sphere. To simulate the behavior of asymmetric dimers we modelled the entity as a sphere cluster consisting of two spheres tangentially attached, the larger sphere is defined as sphere 1 with radius 'r_1' the second sphere is then defined by the size ratio λ so that $r_2 = \lambda r_1$. Knowing the size ratio is critical for defining the dimer's center of diffusion and also for appropriately scaling its diffusion tensor. The diffusion tensor is calculated from Nir and Acrivos [14] work into arbitrary shaped spherical objects; where they write the diffusion tensor as a 6x6 matrix, when the dimer is symmetric only the central diagonal is non-zero. However, for asymmetric dimers the forces on the spheres are unequal resulting in stress build up along the dimer's long axis, the diffusion tensor is then given as:

$$D = \frac{k_B T}{\pi \mu} \begin{bmatrix} a_1 & 0 & 0 & 0 & d_1 & 0 \\ 0 & a_1 & 0 & -d_1 & 0 & 0 \\ 0 & 0 & a_1 + a_2 & 0 & 0 & 0 \\ 0 & -d_1 & 0 & b_1 & 0 & 0 \\ d_1 & 0 & 0 & 0 & b_1 & 0 \\ 0 & 0 & 0 & 0 & 0 & b_1 + b_2 \end{bmatrix}$$

Where the constants are spline fitted from the results of [14], due to the dimer's asymmetry the friction coefficient – which is related to the diffusion coefficient – is different depending on the axis the fluid is flowing parallel to. The Brownian displacements and rotations are generated at random in proportion to the diffusion tensor.

Finding equilibrium positions:

In order to determine the equilibrium trapping locations of an arbitrary multi-sphere cluster we need to be able to compute the optical force at any position and orientation. The optical forces can be computed by a summation of the incident and scattered beam expansion coefficients; the z-axis force is given below:

3. Results and Discussion

Trapping forces on a sphere are often written as the rate of change in momenta of incident and scattered beams [15]. We show in Fig. [1], the axial-force on a single trapped polystyrene microbead of varying radii as the bead is moved along the z-axis computed using the Optical Tweezer Toolbox *ott* under a linearly polarised trap generated with an objective lens of NA 1.2 and wavelength 1064nm. For the case of a dimer, we use *mstm* to compute the scattered fields and *ott* to compute the forces and torques consequent of the scattering processes. It may seem reasonable to write down the force on a dimer as the sum of forces on two beads that make up the dimer with positions of the centre of each bead measured from the beam focus. We put this approximation to test in Fig [2] where we compare it with a rigorous calculation of the force using *mstm* and *ott* and see it fail as soon as the second bead starts being a 10^{th} in radius of the first bead. This makes the case for use of packages like

mstm which are dedicated to computing multi-sphere scattering. We adopt the python codes in [13] to simulate Brownian dynamics of a dimer made of spheres of diameter 0.8micron trapped in a left-circularly polarised light of power 5mW and the spheres are assumed to be made of polystyrene of refractive index 1.58 with water of index 1.33 at 295K as the medium of suspension. Optical forces and torques on this dimer are shown in Fig [3]. and rotation frequency of the dimers as a function of the ratio of the Stokes vector element S_3/S_0 is shown in Fig. [4]. We see very good agreement of these results with those reported in [13].

3.1 Axial forces and Equilibrium positions:

We explore the trapping landscape by plotting out the trapping force as the dimer is moved along the z-axis and see that for the case of large-bead-over-small, there are multiple trapping equilibria compared to the case of small-bead-over-large as seen in Fig [4] and Fig [5]. In all these calculations, we maintain the radius of one of the beads making up the dimer at 1micron and vary the size of the other bead to 500nm, 250nm, and 100nm respectively in the case of size-ratios 1:2, 1:4, and 1:10. In Fig. [6] we plot out the force curve for a symmetric dimer with the size of each sphere equal to 1micron.

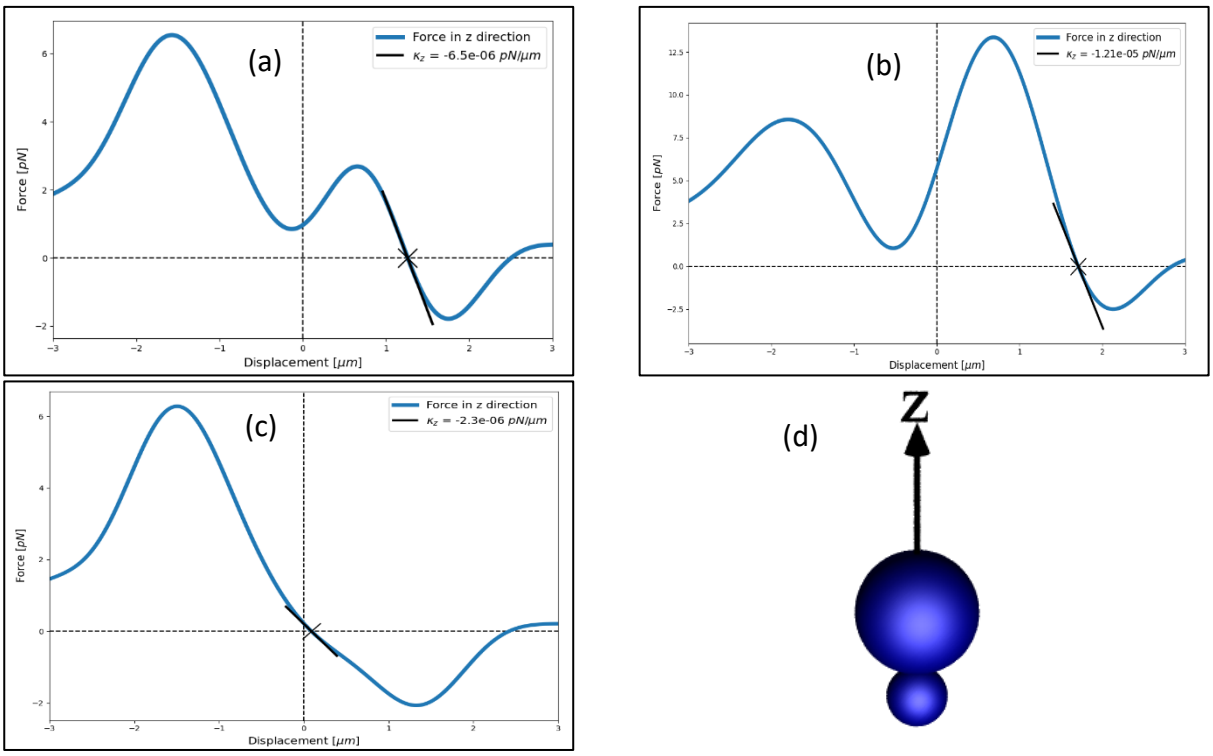

Fig [4]: Plots of force(N) vs displacement of the point of the contact of the spheres(μm) for the case of a dimer with larger bead above the smaller bead when viewed along the positive z-direction – see (d). Size ratios in (a), (b), and (c) are 1:2, 1:4, and 1:10 respectively. The black lines on each force-curve is a linear fit with the slope being reported as the trap stiffness in the legend.

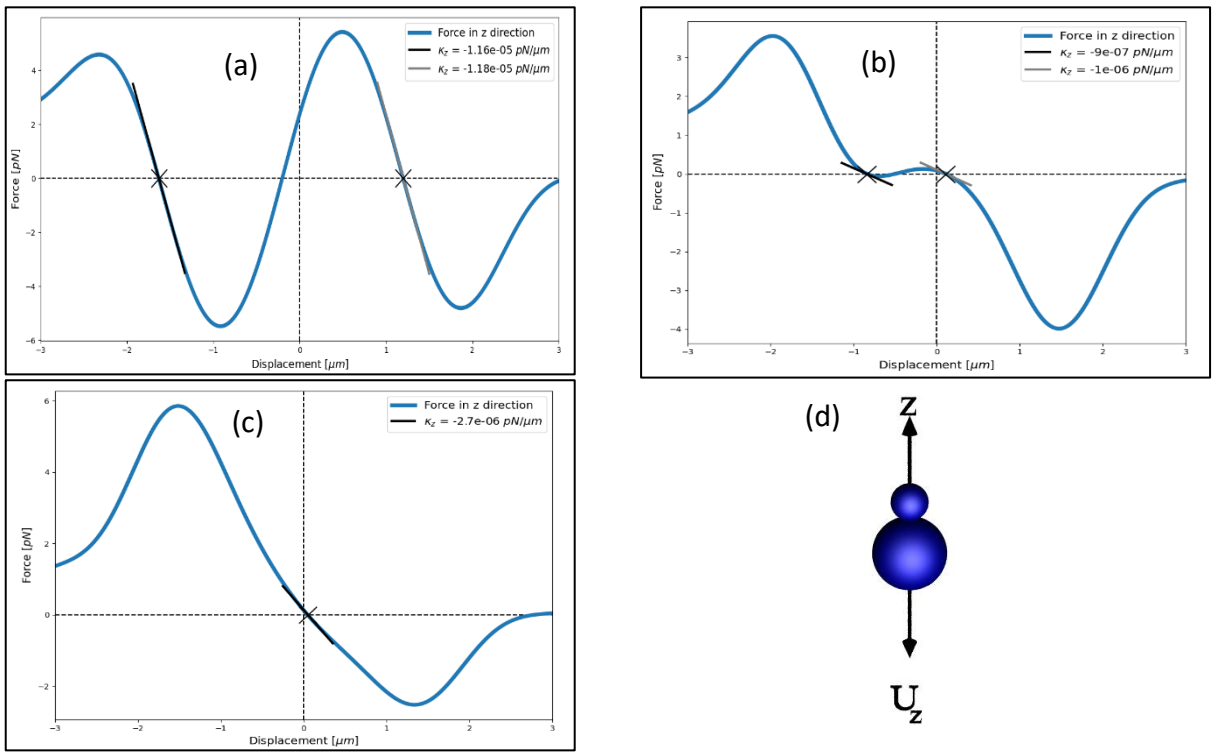

Fig [5]: Plots of force(N) vs displacement of the point of the contact of the spheres(μm) for the case of a dimer with smaller bead above the larger bead when viewed along the positive z-direction - see (d). Size ratios in (a), (b), and (c) are 1:2, 1:4, and 1:10 respectively. The black lines on each force-curve is a linear fit with the slope being reported as the trap stiffness in the legend.

Figure 5 shows that there exists a second trap below the focus of the trapping beam, this trap is only stable when the dimer is orientated against the beam propagation direction. We extend this analysis for size ratios between 1 to 10. Not only is the second trap only possible within the range 1.1 to 4, after which the second trap stiffness goes to 0, the trapping positions as a function of size ratio are shown below.

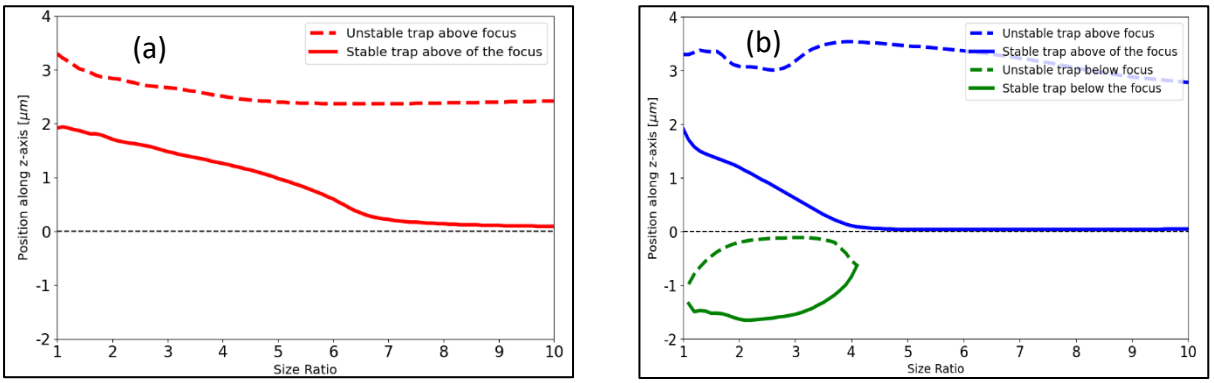

Fig [6]: Plot of trapping positions vs size ratio for (a) dimer orientated with beam propagation direction, and (b) dimer orientated against beam propagation direction. Dashed lines denote the unstable trapping points (only viable for low temperature simulations; solid lines denote stable trapping points.

3.2 Torques and equilibrium orientations:

Having determined the axial-equilibrium positions of the dimers, we go about determining the steady-state orientations of the dimers assuming they've been trapped at their axial-equilibrium positions. The torques reported here are about the X and Y directions of the dimer as discussed in the section on Methods. Fig. [7] shows plots of Torque as a function of angles made with the X and Y axes of a reference frame whose origin coincides with the point-of-contact of the dimer as described in the

section on Methods and the orientation of the dimer is small-over-large looking along the positive z-axis. In Fig 7(a) and Fig 7(b), we show plots of torque vs orientation for a dimer of size-ratio 1:2 at axial positions -1.63µm and 1.2µm respectively. In Fig 7(c) and Fig 7(d), we show torque vs orientation plots for a dimer of size ratio 1:4 at axial positions 0.11µm and -0.84µm respectively and in Fig 7(e) we show torque vs orientation for a dimer of size ratio 1:10 trapped at the focus. In Fig [8] we show torque curves for a symmetric dimer where the microspheres are both assumed to be of radius 1micron. We change the polarisation of light to linear in plots shown in Fig [9]. We assume the light to be polarised along x-axis and see no significant torque along this direction and therefore we only show torque vs angular displacement about y-axis. In Fig. [10], we show these results for a symmetric dimer where the microsphere radius is 1micron.

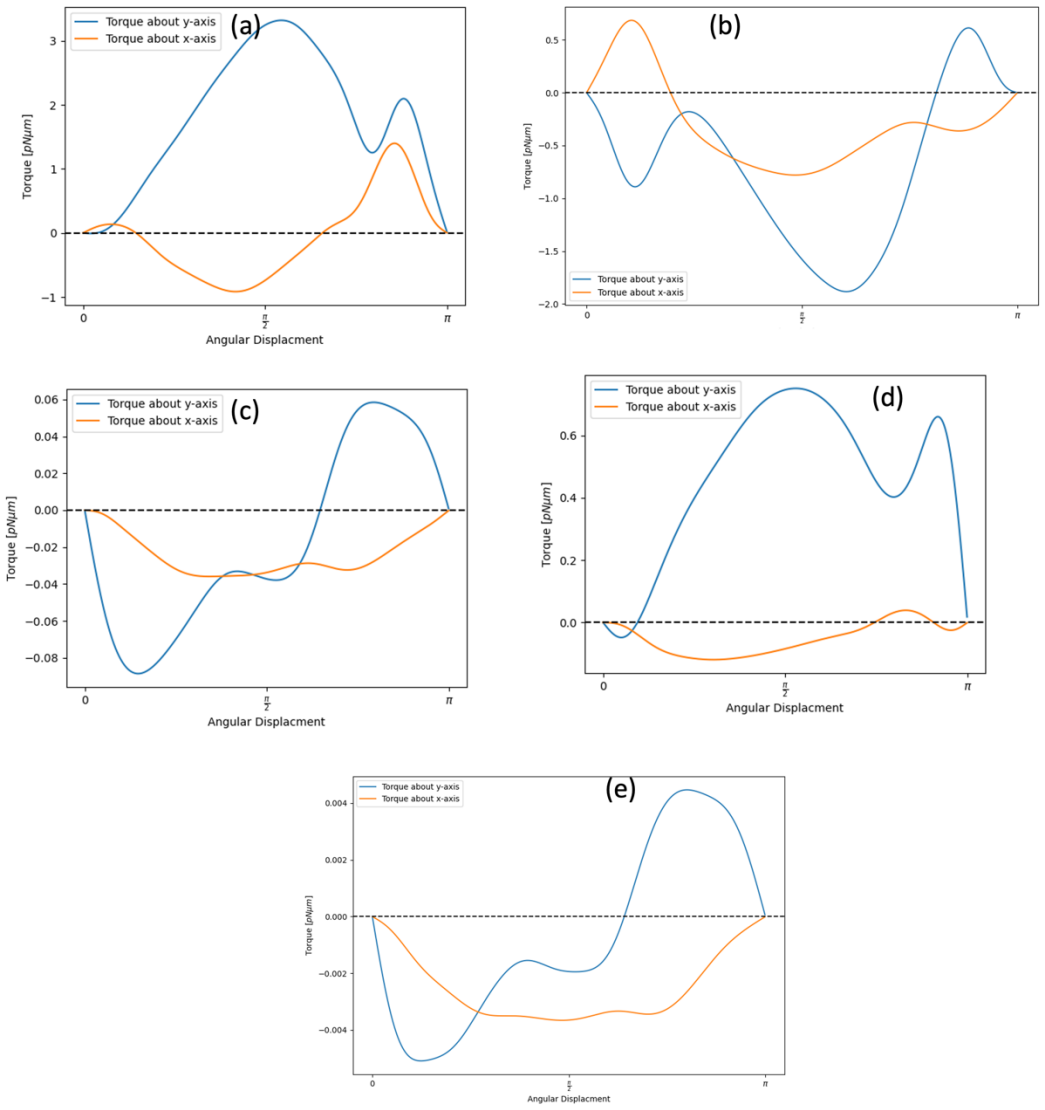

Fig 7: Plots of Torque(pN.µm) vs angular displacement (radian) about X and Y axes of the dimer for size ratios 1:2 in (a) and (b), 1:4 in (c) and (d),and finally 1:10 in (e). The light incident is assumed to be left-circularly polarized and power 5mW. The dimers are assumed to be trapped small-over-large looking down the beam propagation direction. Furthermore, the points-of-contact of the spheres making up the dimer are made coincident with axial equilibrium positions shown in Fig [5].

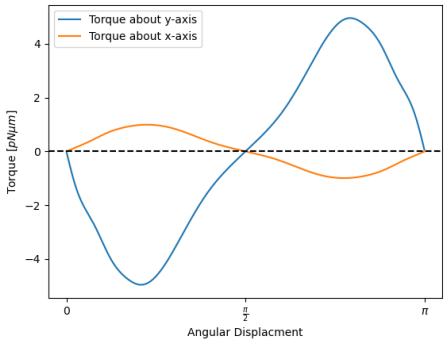

Fig 8: Torque vs orientation along x and y axes of a symmetric dimer where the spheres have a radius of 1µm. The light incident is left circularly polarised and is trapped at its axial equilibrium position of 2µm as seen in Fig [6].

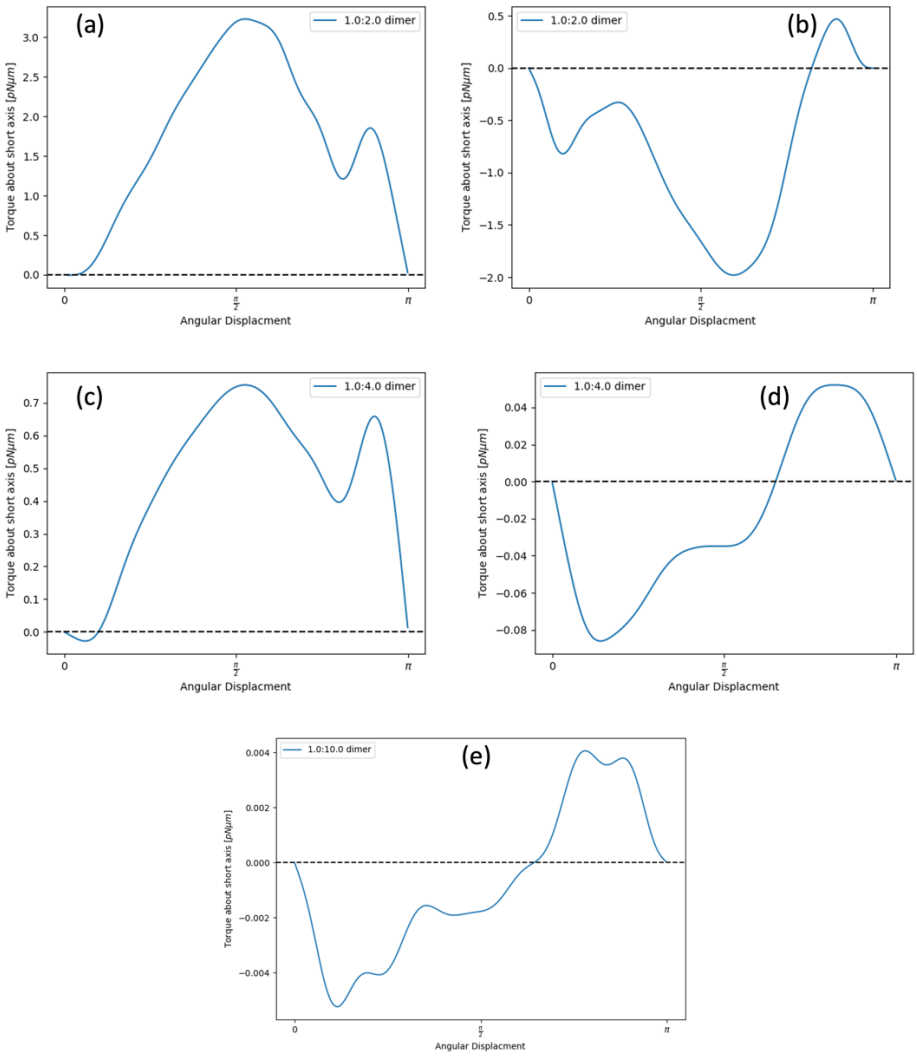

Fig 9: Torque vs angular displacement plots for asymmetric dimers trapped with laser light polarised along the x-direction. Torques shown are for angular displacements about the y-axis, torques about the x-axis are several orders of magnitude smaller in comparison and are therefore not shown. Dimers of size ratio 1:2 are plotted in (a) and (b), 1:4 in (c) and (d), and 1;10 in (e). These are each trapped at their equilibrium z-positions as shown in Fig [5] in the small-over-large orientation looking along positive z-direction.

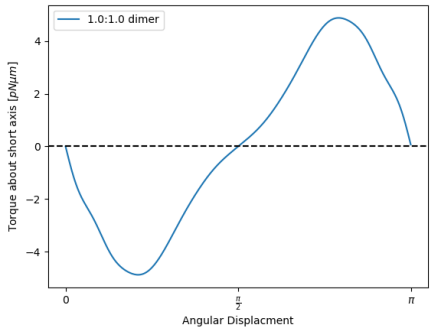

Fig 10: Plot of Torque vs angular displacement about the y-direction for a symmetric dimer in a trap linearly polarised along x-direction. Torque along the laser polarisation direction (x-direction) is several orders of magnitude smaller in comparison and is therefore not shown.

Simpson and Hanna have reported a strong coupling between translational and rotational motion of rod-shaped microscopic particles in an OT [] and we feel it's reasonable to expect a similar effect in case of dimers. Therefore, we probe the stability of the axial-equilibrium to rotations when dimers are rotated after being trapped at their axial equilibrium positions reported in Fig [5]. We therefore plot axial force as a function of displacement about the y-axis when the trap is linearly polarised along x-direction. These are shown in Fig [11].

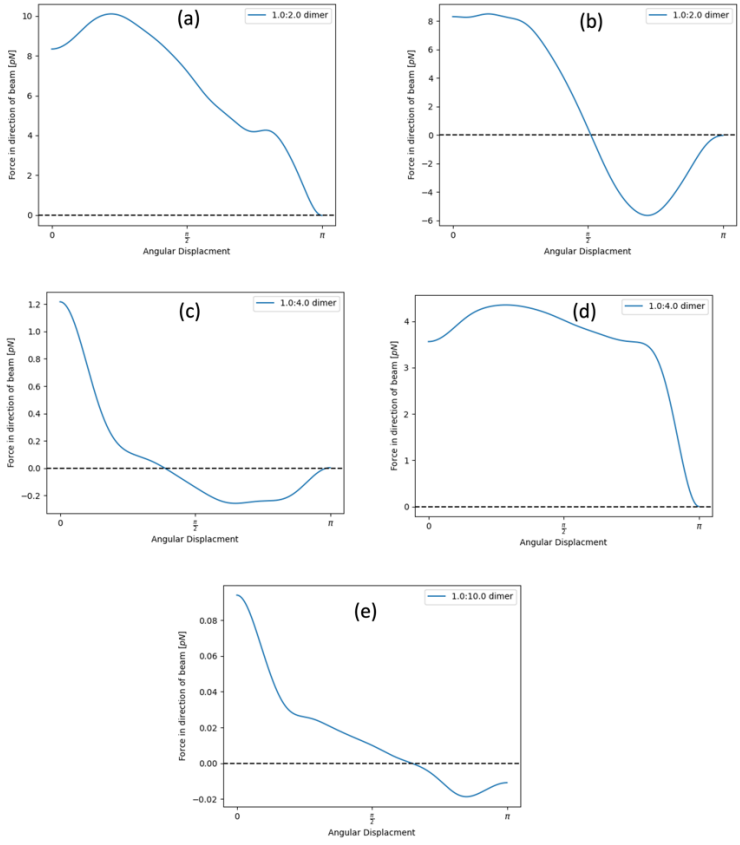

Fig 11: Plot of axial force vs angular displacement for asymmetric dimers when trapped at their axial equilibrium positions as shown in Fig [5]. Dimers of size ratio 1:2 are plotted in (a) and (b), 1:4 in (c) and (d), and 1;10 in (e).

3.3 Rotation Dynamics

Dimers have been shown to rotate within a circularly polarised trap [] meaning they have the potential to be used in micro rotor applications. Interestingly, while the rotation speed is linearly proportional to the laser power it is also dependent on both the orientation and size of the dimer, with the orientation having a greater impact on the rotation speed. We suspect that since the dimer's trapping position is also dependent on the orientation there is a lower transfer of angular momentum when the dimer is closer to the trap focus. This is reflected in Fig 12b where we see the impact of polarization angle on the rotation speed, maximising at 45° and seeing no rotation at 0° and 90°, we simulated dimers of different size ratios with the solid lines representing the rotation speed when the dimer is orientated with the sphere II towards the beam focus and individual points representing the rotation speed when sphere II is orientated away from the beam focus. Despite having the same overall shape and size a 1:4 dimer will not rotate when oriented towards the beam focus, where as the reverse case the dimer rotates at a frequency of roughly 45 Hz.

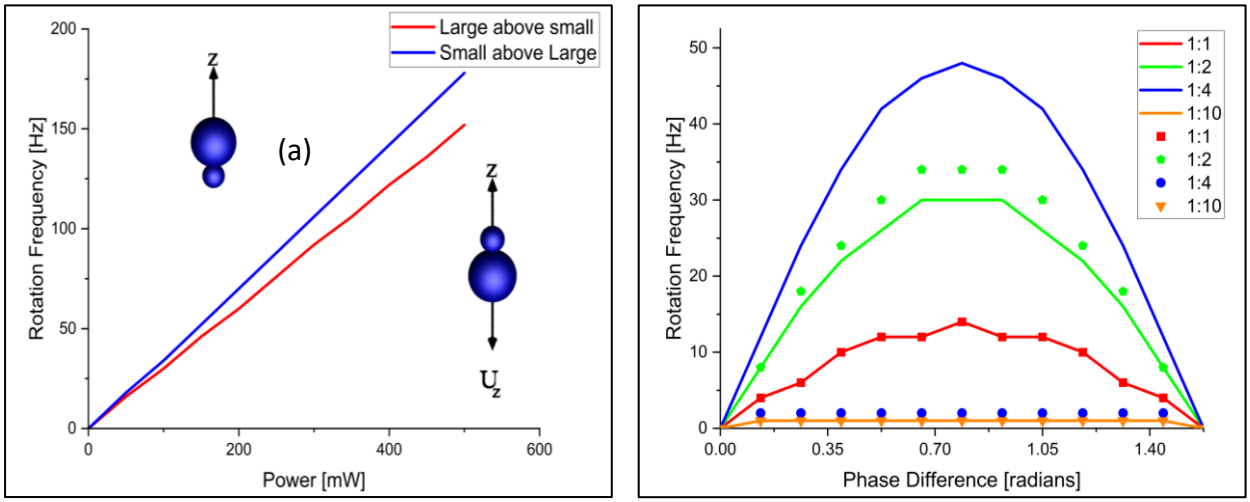

Fig 12: (a) Relationship between laser power and rotation frequency, a dimer of size ratio 2 was simulated in a circularly polarised trap and the rotation speed was measured. On the blue line the smaller sphere is above the larger sphere, whereas for the red line the smaller sphere is below the larger sphere. (b) Relationship between phase difference of the trapping beams Jones Vector, the solid lines are when the smaller sphere is below the larger sphere, individual dots are when the smaller sphere is above the larger sphere.

This is also the case for our second trap below the focus of the beam, in this case we see an even greater rotation rate than above the focus. Interestingly the direction of rotation is flipped upon crossing the focus of the trap, this suggests that the rotations are not induced by a spin-curl effects as these effects are shown to only be caused by the polarisation of the electromagnetic field. We also note that the relationship is also somewhat related to the dimer's displacement from the trap focus, where a greater displacement results in a faster rotation rate, where in each case as soon as the dimer is trapped at the focus the rotation frequency goes to 0.

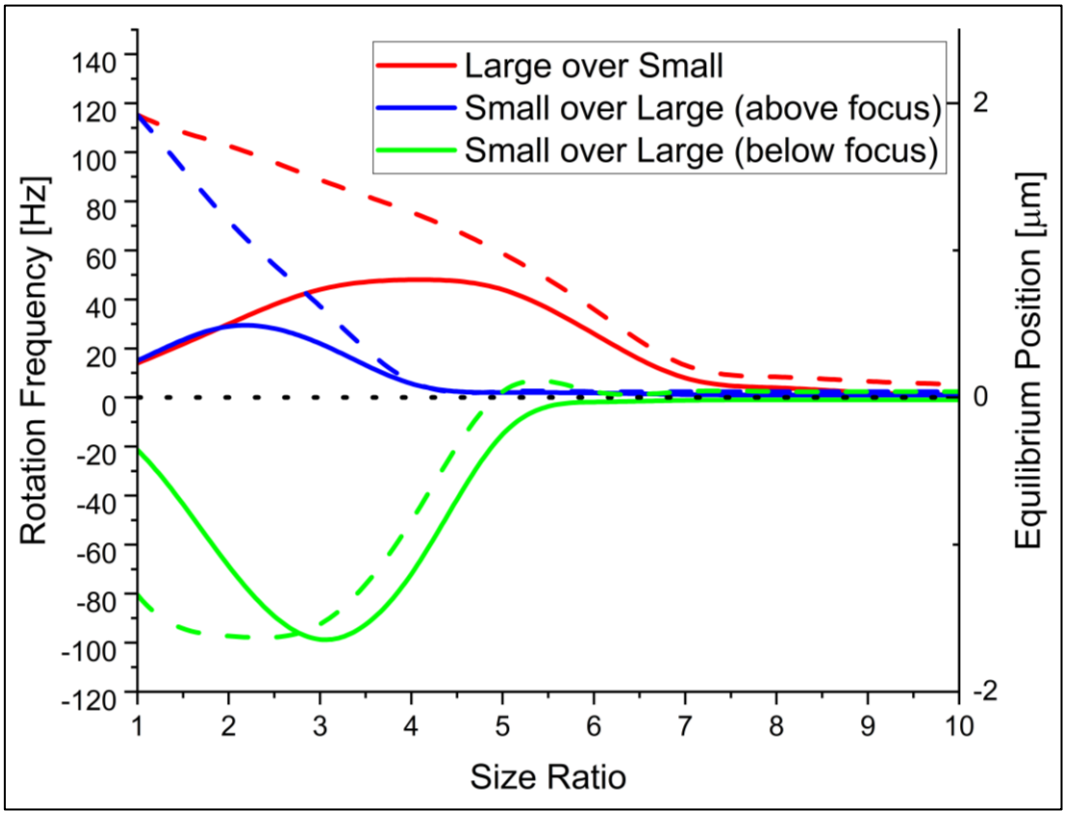

Fig 13: Relationship between dimer size and rotation frequency, red line indicates how the dimer's rotation frequency changes with the smaller sphere orientated away from the trap focus, blue line indicates the same dimer but now rotated 180^0 and still kept above the trap, and the green line indicates the same relationship but now the dimer is situated below the trap focus. Dotted lines represent the distance from the trap focus where the dimer is stably trapped.

Conclusions and Outlook

We study by means of computer simulations, the orientation dependent trapping landscapes for asymmetric microsphere dimers in both linearly and circularly polarized traps and show that trapping with circularly polarized light can lead to sustained rotations that go roughly as 0.25 Hz/mW for the orientation of small sphere over large when viewed opposite to the beam propagation direction. These results should provide insights with regards development of experiments probing the trapping behaviour of dimers and also make for interesting comparisons with other complex shapes such as ellipsoids and rods. Furthermore, we hope our results might be useful for development of micro-rotors for lab-on-a-chip assays.

References

[1] A. Ashkin, J.M. Dziedzic, J. E. Bjorkholm, S. Chu, Observation of a single-beam gradient force optical trap for dielectric particles, Opt. Lett 11(5) (1986) 288-290

[2] R. Di Leonardo, R. Keen, F. Ianni, J. Leach, M. J. Padgett, G. Ruocco, Hydrodynamic interactions in two dimensions, Phys. Rev. E 78 (2008) 031406

[3] T. P. Kohler, C. M. Brotherton, A. M. Grillet, Comparison of interparticle force measurement techniques using optical trapping, Colloids Surf A 384 (2011) 282-288

[4] A. Curran, M. P. Lee, M. J. Padgett, J. M. Cooper, R. Di Leonardo, Partial Synchronization of stochastic oscillators through hydrodynamic coupling, Phys. Rev. Lett 82 (1999) 4352-4355

[5] M. Atakhorrami, J. I. Sulkowska, K. M. Addas, G. H. Koenderink, J. X. Tang, A. J. Levine, F. C. MacKintosh, C. F. Schmidt, Phys. Rev. E 73 (2006) 061501

[6] M. Li, J. Arlt, Trapping multiple particles in single optical tweezers, Opt. Comm 281(1) (2008) 135-140

[7] S. Xu, Y. Li, L. Lou, Axial optical trapping forces on two particles trapped simultaneously by optical tweezers, Appl. Opt 44(13) (2005) 2667-2672

[8] X. Sheng-Hua, L. Yin-Mei, L. Li-Ren, S Zhi-Wei, Computer simulation of the collision frequency of two particles in optical tweezers, Chin. Phys 14(2) (2005) 382-385

[9] P. Praveen, Yogesha, S. S. Iyengar, S. Bhattacharya, S. Ananthamurthy, Appl. Opt. 55(3) (2016) 585-594

[10] B. M. Mihiretie, P. Snabre, J. -C. Loudet, B. Pouligny, Optically driven oscillations of ellipsoidal particles. Part I: Experimental observations, Eur. Phys. J. E 37:124 (2014)

[11] Y. Cao, A. B. Stilgoe, L. Chen, T. A. Nieminen, H. Rubinsztein-Dunlop, Opt. Exp 20(12) (2012) 12987-12996

[12] D. Chetana, P. Praveen, B. V. Nagesh, S. Bhattacharya, S. Ananthamurthy, J. Opt 24(9) (2022) 094007

[13] W. Vigilante, O. Lopez, J. Fung, Opt. Exp 28(24) (2020) 36131-36146

[14] D. W. Mackowski, M. I. Mishchenko, A multiple sphere T-matrix Fortran code for use on parallel computer clusters, J. Quant. Spectrosc. Radiat. Transfer 112(13) (2011) 2182-2192

[15] T. A. Nieminen, V. L. Y. Loke, A. B. Stilgoe, G. Knöner, A. M. Branczyk, N. R Heckenberg, H Rubinsztein-Dunlop, J. Opt A-Pure Appl.Opt 9 (2007) S196-S203

Appendices

Determining Rotation Rate

Computing the rotation frequency of a rotating dimer is a simple enough computation, as mentioned in section 2, the dimer has three primary reference axis, U_x U_y, and U_z. While the latter defines the main orientation of the trapped dimer the former two define the x-y plane which the dimer rotates in. At a sufficiently high laser power (< 100 mW) the motion of these two reference axis will sinusoidally oscillate in the x-y plane, we can take the Fourier transform of this motion to get a power spectral density that is peaked at the fundamental frequency of rotation. This is a similar approach to taking the Fourier transform from QPD data for a birefringent particle but since the spheres are both non-birefringent the scattering would not show this rotation.